Scientific Research Publishing

Geomaterials, 2021, 11, 23-41
https://www.scirp.org/journal/gm
ISSN Online: 2161-7546
ISSN Print: 2161-7538

Depth and Structural Parameters Determination of the Sedimentary Basin in Atmur Nuqra Area, South Eastern Desert, Egypt Using Aeromagnetic Data Analysis

Ahmed A. Elhusseiny, Asmaa A. Azzazy

Nuclear Materials Authority, Cairo, Egypt
Email: ahmednoureldin1985@gmail.com

How to cite this paper: Elhusseiny, A.A. and Azzazy, A.A. (2021) Depth and Structural Parameters Determination of the Sedimentary Basin in Atmur Nuqra Area, South Eastern Desert, Egypt Using Aeromagnetic Data Analysis. *Geomaterials*, **11**, 23-41.
https://doi.org/10.4236/gm.2021.112002

Received: February 15, 2021
Accepted: March 29, 2021
Published: April 1, 2021

Abstract

The study area is located at the south of the eastern desert of Egypt between latitudes 24˚N to 25˚N and longitudes 33˚E to 33˚50'E covering an area of about 9407 km^2. The study area is mainly covered with sediments whose age extends from the upper Cretaceous to the Quaternary, in addition to the presence of some basement rocks such as younger granites, metasediments and metagabbro. The research aims essentially to determine the thickness of the sedimentary basin by determining the depth to the top of basement and delineating the subsurface geological structures which affected this sedimentary basin. The Euler depth map exhibited that the north parts of the area have shallow depth values from 1000 m to 2000 m. The southern parts also show a shallow to moderate depths ranging from 1000 m to 2400 m. The deepest parts are located at the middle and at the western parts and are ranging in value from 3000 m to more than 4000 m. The horizontal derivative and tilt derivative techniques proved that the most effective trends all over the study area are NW-SE and NE-SW directions as mentioned in geologic lineaments map. The basement tectonic map shows clearly all the faults affected the area. It shows that there are many high blocks trending mainly in NW-SE and NE-SW directions. All high blocks surround a large sedimentary basin reaches depth of about more than 4000 m. All the results produced from 2D-modeling illustrate that the sedimentary basinal area (G2) is the deeper basin all over the area and it is controlled by some faults and fractures. 3D inversion was used and resulted in that the area of study have many high blocks at shallow to moderate depths which surrounding a large sedimentary basinal area with very deep depth values. All the techniques which applied in this research led to that the largest sedimentary basin is located at the center of the

study area with NW-SE trend and depth value of about 4000 m.

Keywords

Subsurface Structure, Depth to Basement, Magnetic Interpretation, Atmur Nuqra Area, Eastern Desert

1. Introduction

The present study area (**Figure 1**) is located at the southern part of the Eastern Desert of Egypt (covering an area of 9407 km^2). This area is mainly covered by sedimentary rocks ranging in age from Upper Cretaceous to Quaternary. However, there are parts covered by basement rocks. **Figure 1** also shows the topographic features of the present study area. The area ranges in height from 350 m to 700 m at the NE part and southern part of the study area, whereas the map shows that the western part ranges in height from 90 m to 230 m extending from

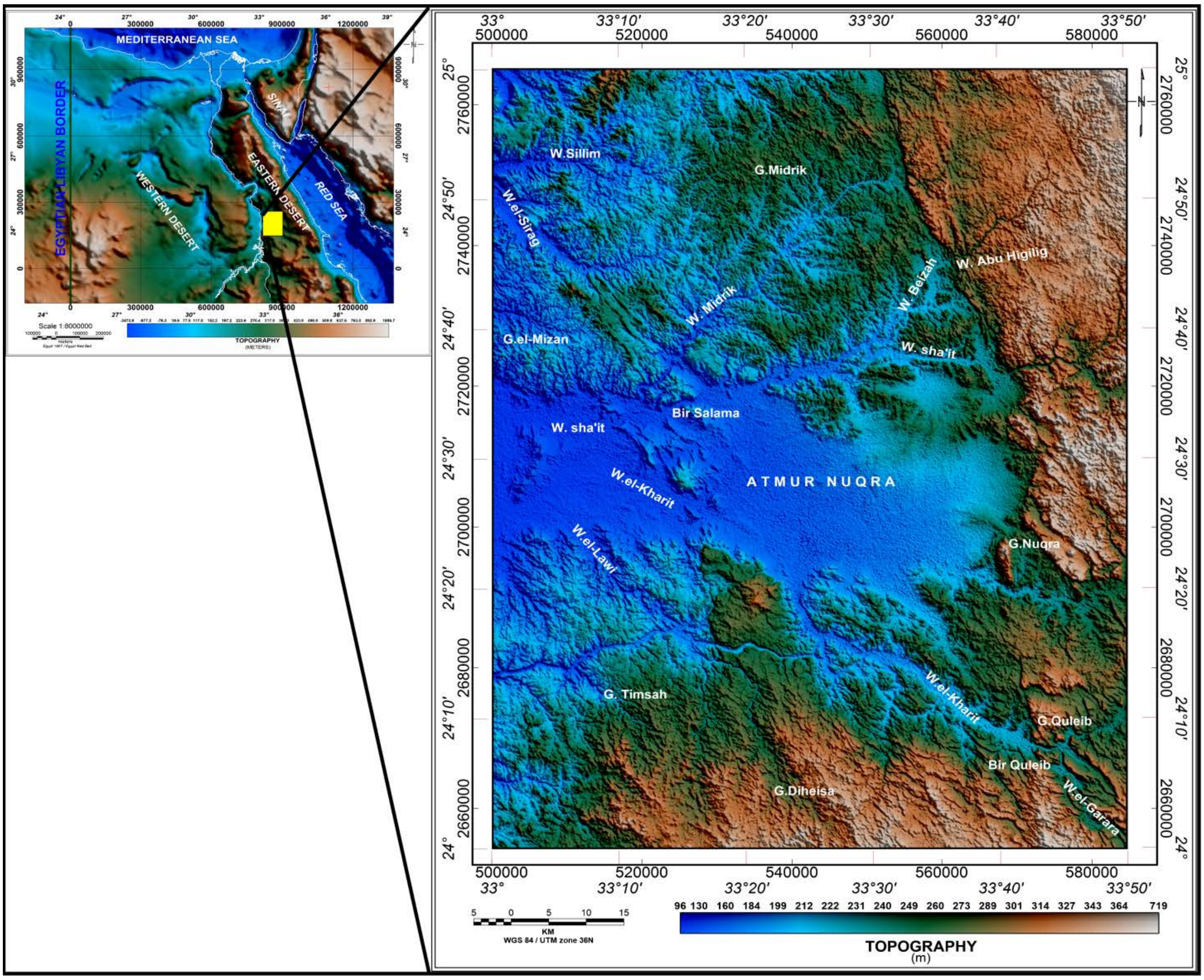

Figure 1. Location and topographic map of Atmur Nuqra area, South Eastern Desert, Egypt.

north to the middle of the area.

To achieve the main goal of this research, which is to determine the depth and thickness of the sedimentary basin by determining the depth to basement, many modern techniques have been applied, such as calculating the basement depth with Euler Deconvolution method. In addition, 2D and 3D-aeromagnetic models were used also to determine the depth of basement and hence the thickness of the sedimentary basin. Another objective is to detect the subsurface structural features that control this sedimentary basin. For achieving this objective, horizontal derivative and tilt derivative were applied. All techniques were used in an integrative manner to achieve the objectives of the study.

2. Regional Geology

The study area is a part of the Eastern Desert of Egypt. Eastern Desert can be described as largely occupied by an association of metasediments, metavolcanics, metagabbro and serpentinites consisting the ophiolitic mélange [1]. The study area exhibits also wide range of sedimentary rocks which extend in age from upper cretaceous to quaternary (**Figure 2**).

Abu Aggag formation overlain the basement at the south of Wadi El-kharit area and composed mainly of fluviatile sandstone and ripple laminated sandstone. This formation is overlained by Taref formation which composed mainly of fluviatile and eolian sandstone, fine to medium grained with interbedded channel and soil deposits. Timsah formation is lying over Taref formation at the study area and consists of deltaic sequence of shale, silt, and sandstone with two major oolitic iron-ore beds, typically 10 - 15 m and carrying frequent fossil plants. This formation is overlained by Umm-Barmil formation which is fluviatile sandstone becoming more marine towards the north [2]. Quseir clastics are made of detrital quartz and dolomite with iron oxide and phosphatic remains in the form of plates. The Nubia sandstone is followed by Quseir variegated shale of Campanian age. This formation is composed mainly of poorly fossiliferous variegated shales and clays deposited under none-marine to marginal marine conditions. The Quseir variegated shale is overlain by Duwi Formation which is made up of three phosphate horizons separated by beds of black shale, marl, and oyster limestone. Duwi Formation is followed by Dakhla Formation which is represented by dark grey shallow marine marl and shale with limestone intercalations [2].

Dakhla shale is overlain by a carbonate bed which is recognized with ease due its sharp contact with the overlying and underlying dark green shales. This carbonate bed is equivalent to Tarawan chalk of the western Desert oases which is made up of marl and marly limestone. Tarawan Formation is overlain by Pliocene deposits which are in the form of fluviatile siltstone, sandstone, and claystone [2]. Detritus, sands, gravels, pebbles, cobbles, and boulders are distributed all over the area and constitute the surficial cover in the main Wadis. They are generally formed by the weathering of different types of rocks. This cover represents

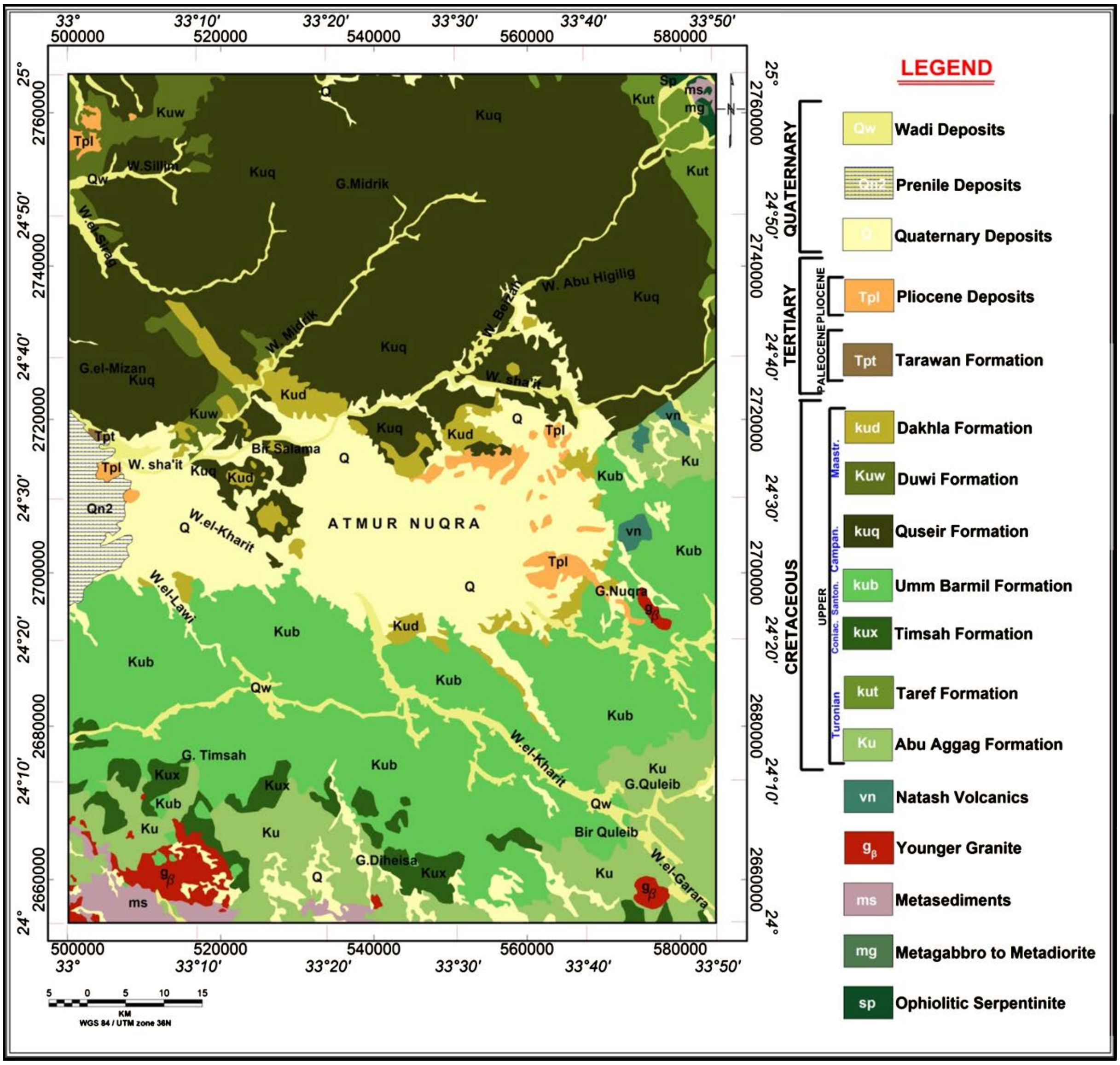

Figure 2. Regional geological map of Atmur Nuqra area, South Eastern Desert, Egypt, (Reproduced after Conco Coral and EGPC, 1987).

Quaternary age sediments (Figure 2).

The Eastern Desert of Egypt lies within the fold and thrust belt of the Pan-African continental margin orogeny [3]. It consists of relatively thin and imprecated thrust sheets overlying an attenuated Early Proterozoic continental margin. Two tectonic trends namely NW-SE and NE-SW prevail in the Eastern Desert of Egypt. [4] [5] [6] believed that the Pan African belt was created by compression from an easterly direction, while [1] [7] and [8] consider that the direction of tectonic transport was towards the NNW. The distribution of major rock units shows that the study area is composed of large fragments separated by major zones of tectonic dislocations [9]. According to the constructed structural map [9], the fracture lineaments including faults have two main trend sets: NW-SE and NE-SW (Figure 3).

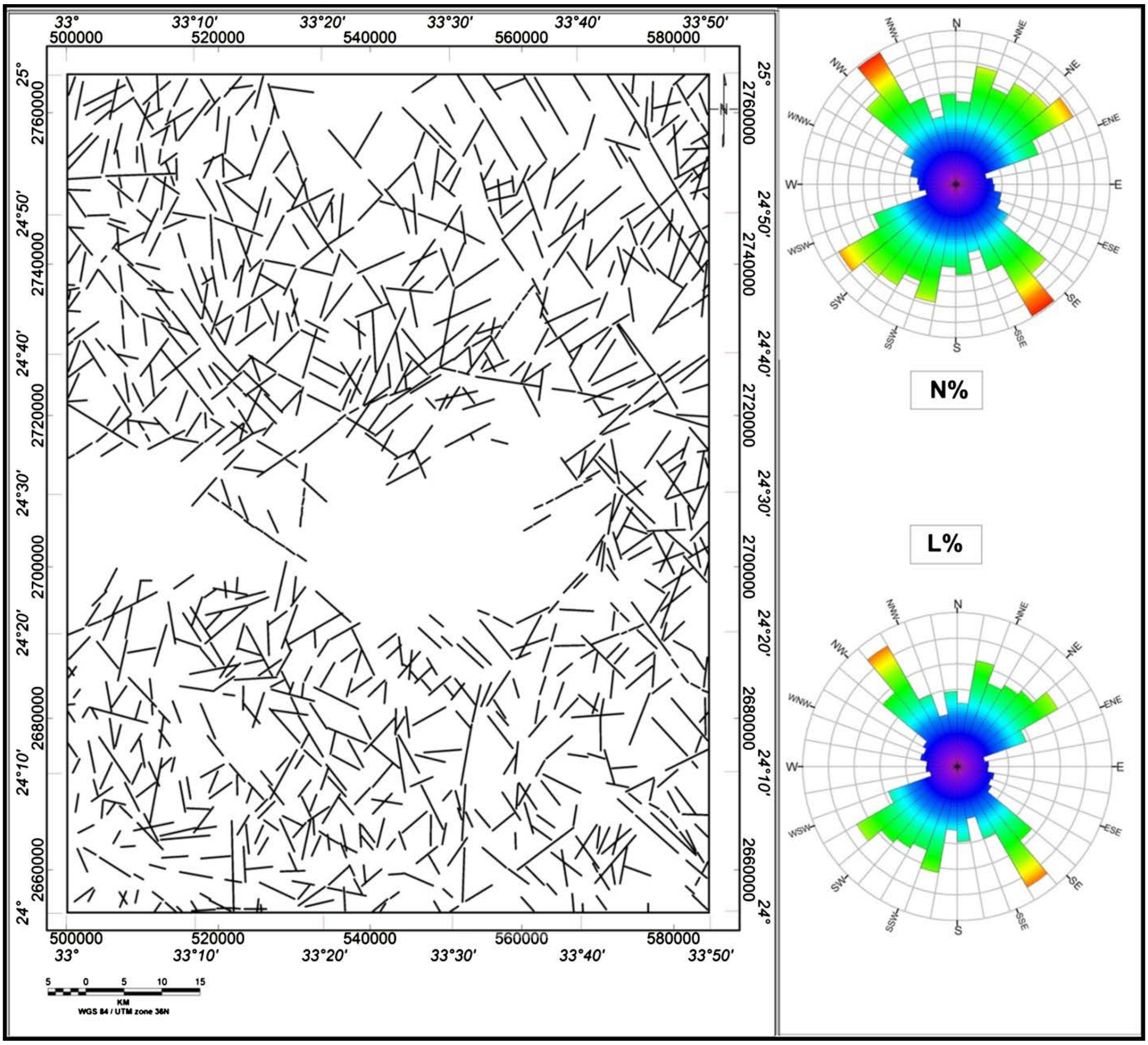

Figure 3. Structural geological lineaments map (Reproduced after Conco Coral and EGPC, 1987) and its rose diagram of Atmur Nuqra area, South Eastern Desert, Egypt.

3. Aeromagnetic Data

In 1984, Aero-Service Division, Western Geophysical Company of America conducted high resolution magnetic survey covering an area of 9407 km^2 over the study area (**Figure 1**). The data were acquired along flight-lines oriented in NE-SW direction using 1.5 Km line spacing and along tie-lines oriented in NW-SE direction using 10,000 m line spacing. Nominal flying elevation was 120 m above ground surface [10] (**Figure 4**).

4. Interpretation

The reduced to north pole magnetic (RTP) map (**Figure 5**) was produced from total intensity magnetic map through applying the spectral analysis to overcome the Bi-Polarity problem. RTP map is filtered and separated into two magnetic

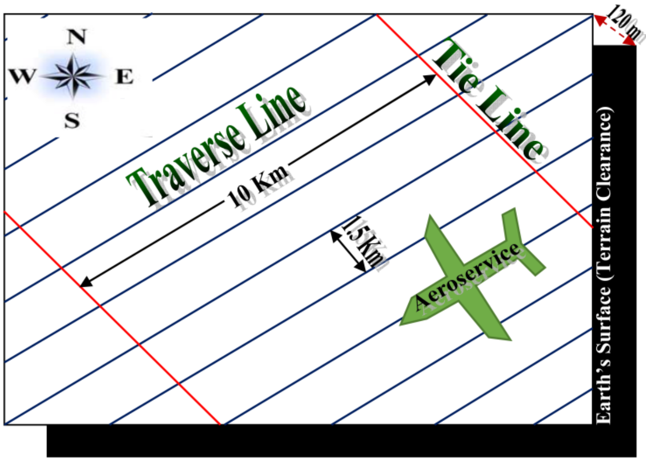

Figure 4. Flight path specifications of the study area (After Aero-service, 1984).

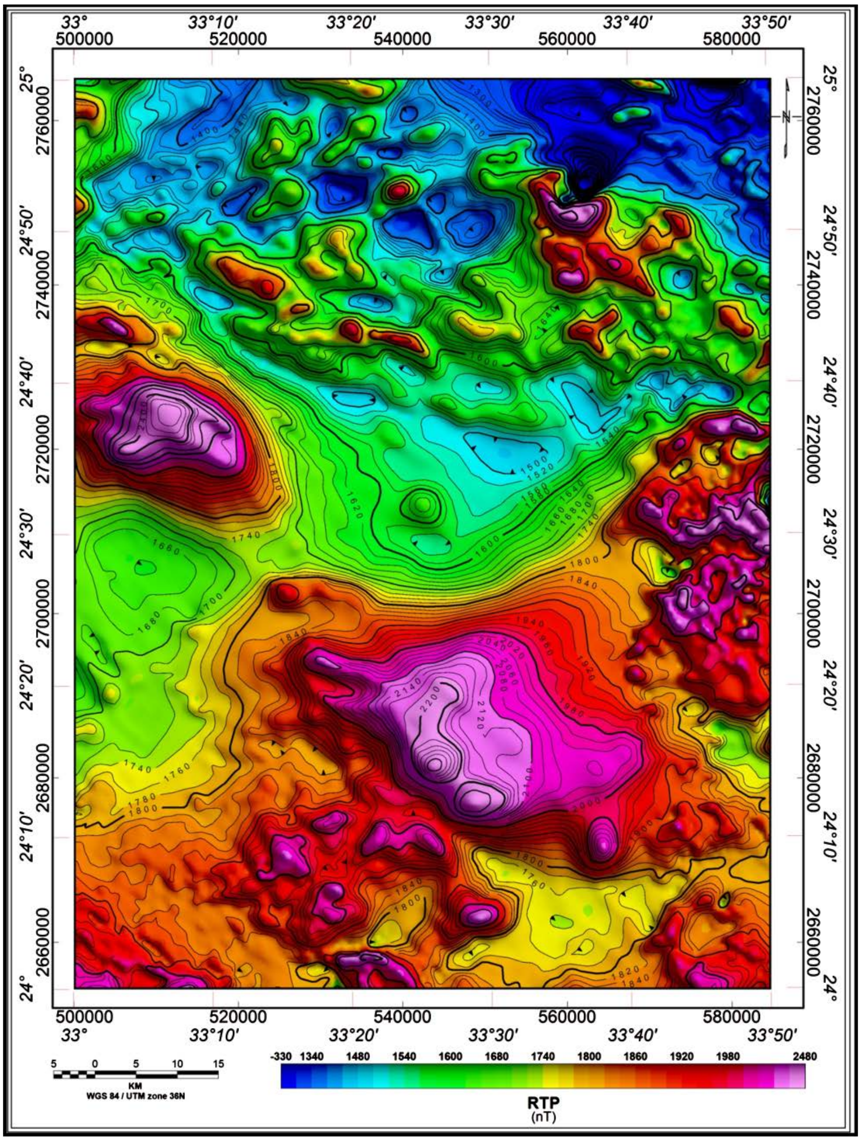

Figure 5. Colour contour map of reduced to the north magnetic pole (RTP) aerial total intensity magnetic field of Atmur Nuqra area, South Eastern Desert, Egypt.

maps named the regional and residual magnetic components (Figure 6 & Figure 7). The estimated mean depths of both the regional and residual magnetic sources were found to be 4200 m and 1800 m, respectively.

RTP map (Figure 5) shows a positive anomaly at the southern part of the study area with values ranging from 1900 nT to 2480 nT. The map exhibits also other positive anomalies at the eastern and western central parts of the study area with values of about 2400 nT. There is also a negative anomaly at the northern part of the map with value of about −350 nT.

The regional magnetic component map (Figure 6) shows that there are some positive anomalies spreading all over the study area. The positive anomalies are located mainly at the eastern part and extending to southwest direction forming a positive trend in NE-SW direction. Another positive anomaly on regional map

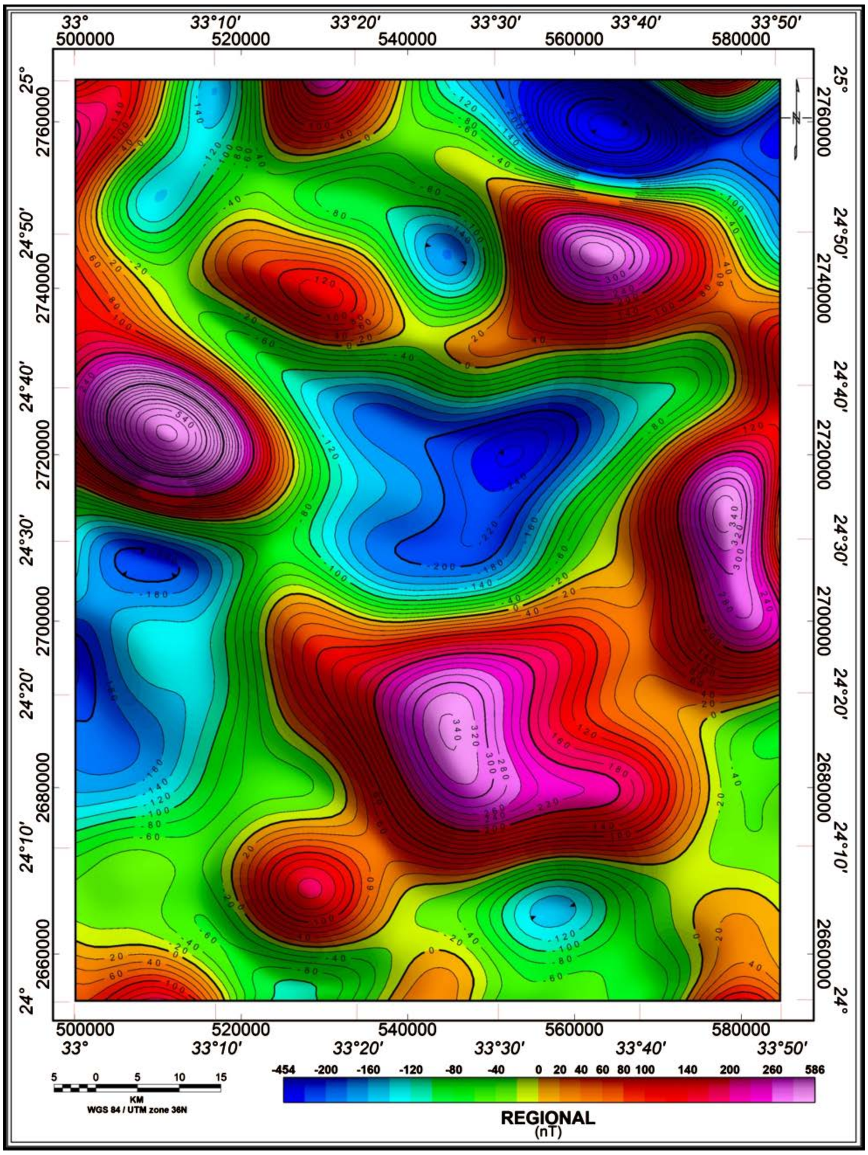

Figure 6. Colour contour map of reduced to the north magnetic pole (RTP) regional magnetic component of Atmur Nuqra area, South Eastern Desert, Egypt.

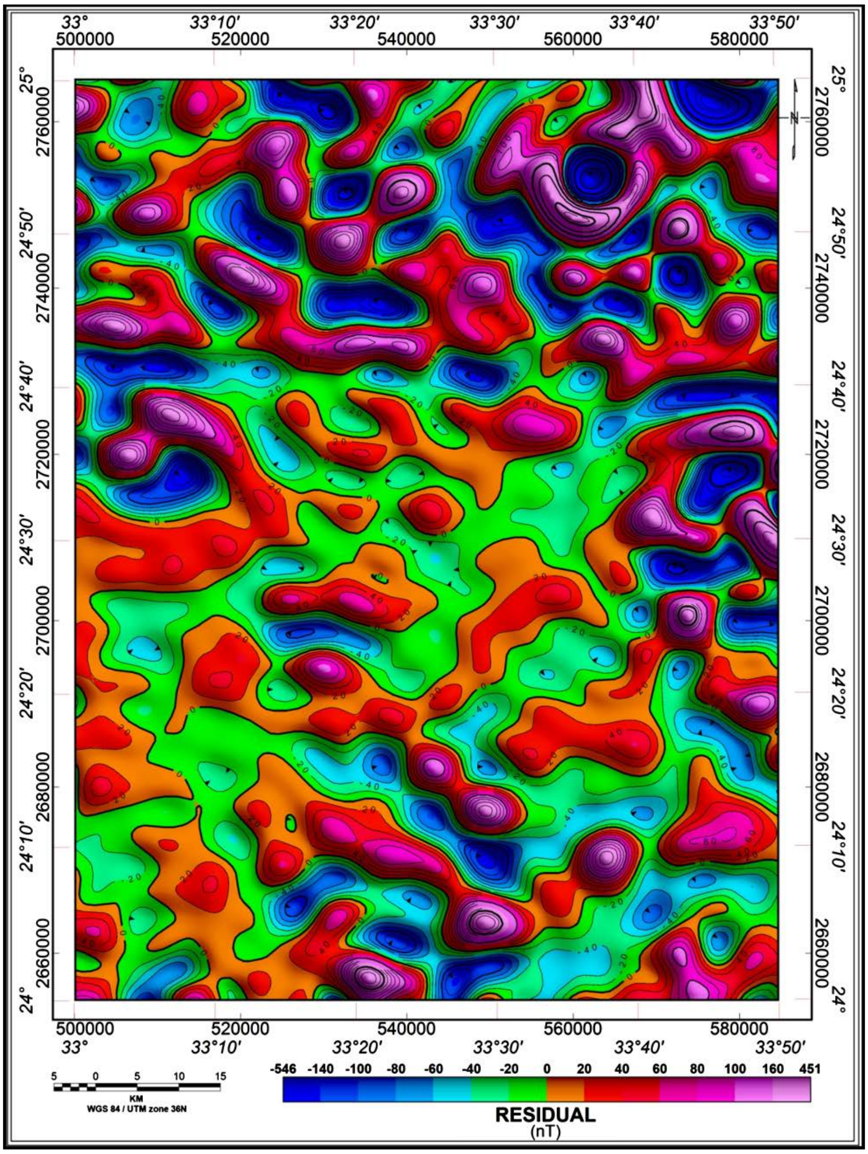

Figure 7. Colour contour map of reduced to the north magnetic pole (RTP) residual magnetic component of Atmur Nuqra area, South Eastern Desert, Egypt.

is located at the western and at the northeastern parts forming another trend close to ENE-WSW direction. Regional Map also exhibits three main negative anomalies; one at the northeastern corner, the second in the central and the third at the western part of the study area. In addition, there are another small negative anomaly located at the northwestern and southern parts. The three main negative anomalies together form a trend close to NE-SW direction.

The residual magnetic component map (Figure 7) demonstrates more about the magnetic-rock types, their contacts and their over-all relationships including faulting, folding, etc., particularly at the near-surface shallow level.

4.1. Discussion of Euler Depth Map

Euler deconvolution method is an automatic technique used for locating the source of potential field based on both their amplitudes and gradients. The method was developed by [11] to interpret the 2D magnetic anomalies and extended by [12] to be used on grid-based data. Magnetic field M and its spatial derivatives satisfy Euler's equation of homogeneity.

$$(x-x_0)\frac{\partial M}{\partial x}+(y-y_0)\frac{\partial M}{\partial y}+(z-z_0)\frac{\partial M}{\partial z}=-NM$$

Where $\frac{\partial M}{\partial x}$, $\frac{\partial M}{\partial y}$ and $\frac{\partial M}{\partial z}$ represent first-order derivative of the magnetic field along the *x*-, *y*- and *z*-directions, respectively, N is known as a structural index and is related to the geometry of the magnetic source [12].

The depths of anomalies in the study area were calculated through applying euler method with structure index N = 1 (**Figure 8**). The euler depth map clearly

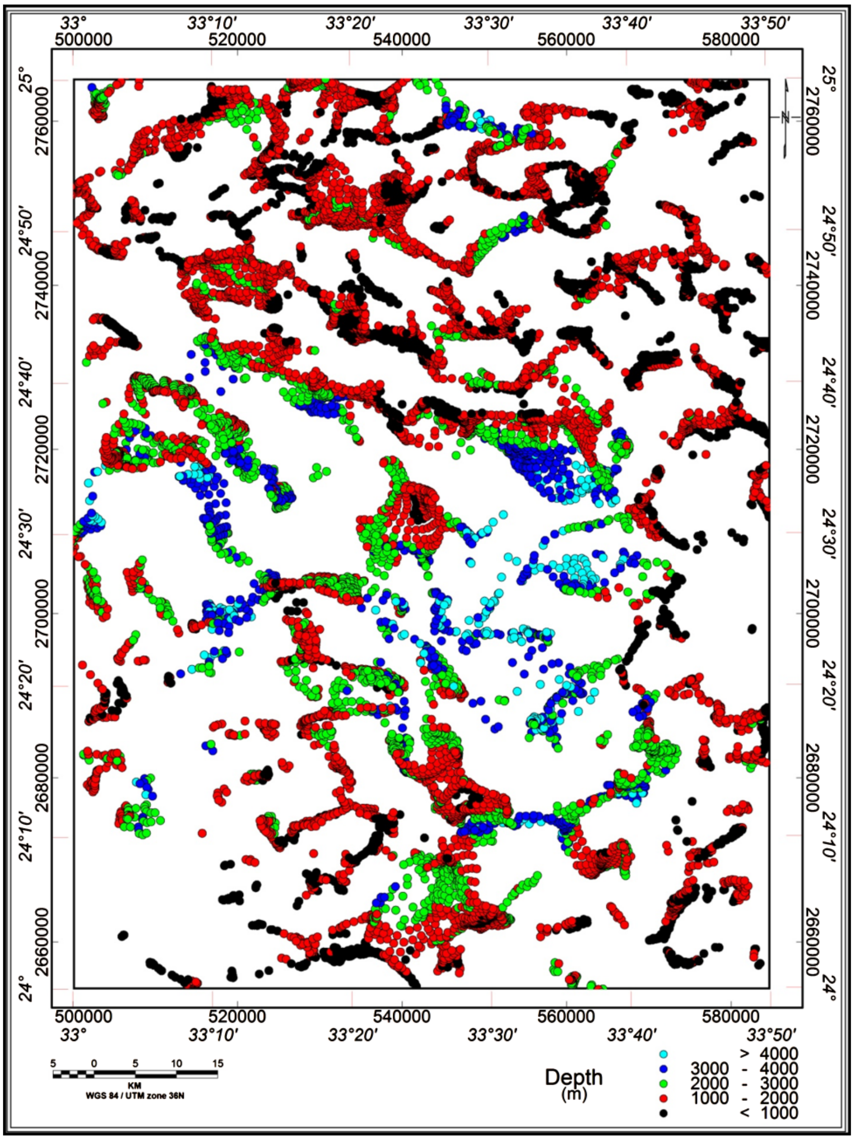

Figure 8. Euler depth solution map of reduced to the north magnetic pole (RTP) with N = 1 of Atmur Nuqra area, South Eastern Desert, Egypt.

shows that the northern part of the area exhibits shallow depth values. These values range from 1000 m to 2000 m. The southern parts also show a shallow to moderate depths ranging from 1000 m to 2400 m. The deepest values are located at the central and at the western parts of the study area which may indicate the presence of large basins. The depths at these parts are ranging in values from 3000 m to more than 4000 m. The euler map not only shows the depth variations through the area but also shows the trends that affect the area. The map shows two main trends in NE-SW and NW-SE directions (**Figure 8**).

4.2. Discussion of Basement Structural Trends

To highlights the geological structures that affecting on the study area and the formation of sedimentary basins, total horizontal derivative and tilt derivative techniques were applied to the regional and residual magnetic components. Regional and residual structural lineaments were traced over horizontal derivative and tilt derivative grids to illustrate the structural trends affecting the study area (**Figure 9** & **Figure 10**). Rose diagram of regional lineaments show that the WNW-ESE trend is the most effective trend at deeper depths all over the area.

The residual lineaments rose diagram show that there is more than one effective trend. These trends can be arranged in terms of their effect as follow; NW-SE, WNW-ESE, and NE-SW trends. All these trends are effective at shallow to moderate depths all over the study area.

The regional and residual lineament trends (**Figure 9** & **Figure 10**) agree with the geology lineament trends (**Figure 3**) that the most effective trends in the area under consideration include two major sets of trends: NW-SE trend (Gulf of Suez trend) and NE-SW trend (Gulf of Aqaba trend). With the integration of all aforementioned magnetic maps, a basement tectonic map (**Figure 11**) was constructed to illustrate the main faults affected the study area.

4.3. Discussion of Basement Tectonic Map

Basement tectonic map (**Figure 11**) was constructed through the analysis of regional, residual, horizontal derivative, tilt derivative and euler maps. The map shows that the area is affected by some normal faults directed mainly in NE-SW and NW-SE direction. The area also suffered from strike-slip movements; mainly in NNW-SSE direction and other small strike-slip movements in ENE-WSW direction. All the strike-slip movements separate the narrower high blocks from the broader high blocks.

Basement tectonic map (**Figure 11**) shows that there are some high blocks (Horst) denoted on the map as (H1) to (H16) separated by basinal areas (Graben) denoted on the map as (G1) to (G4). At the north western part of the area, there are three high blocks (H1 to H3) which detected at shallow to moderate depths and trend in NE-SW direction. To the south of these three blocks, there are four high blocks (H4 to H7) detected at shallow depths and all are trending in approximately NW-SE direction. All high blocks at the north from (H1) to

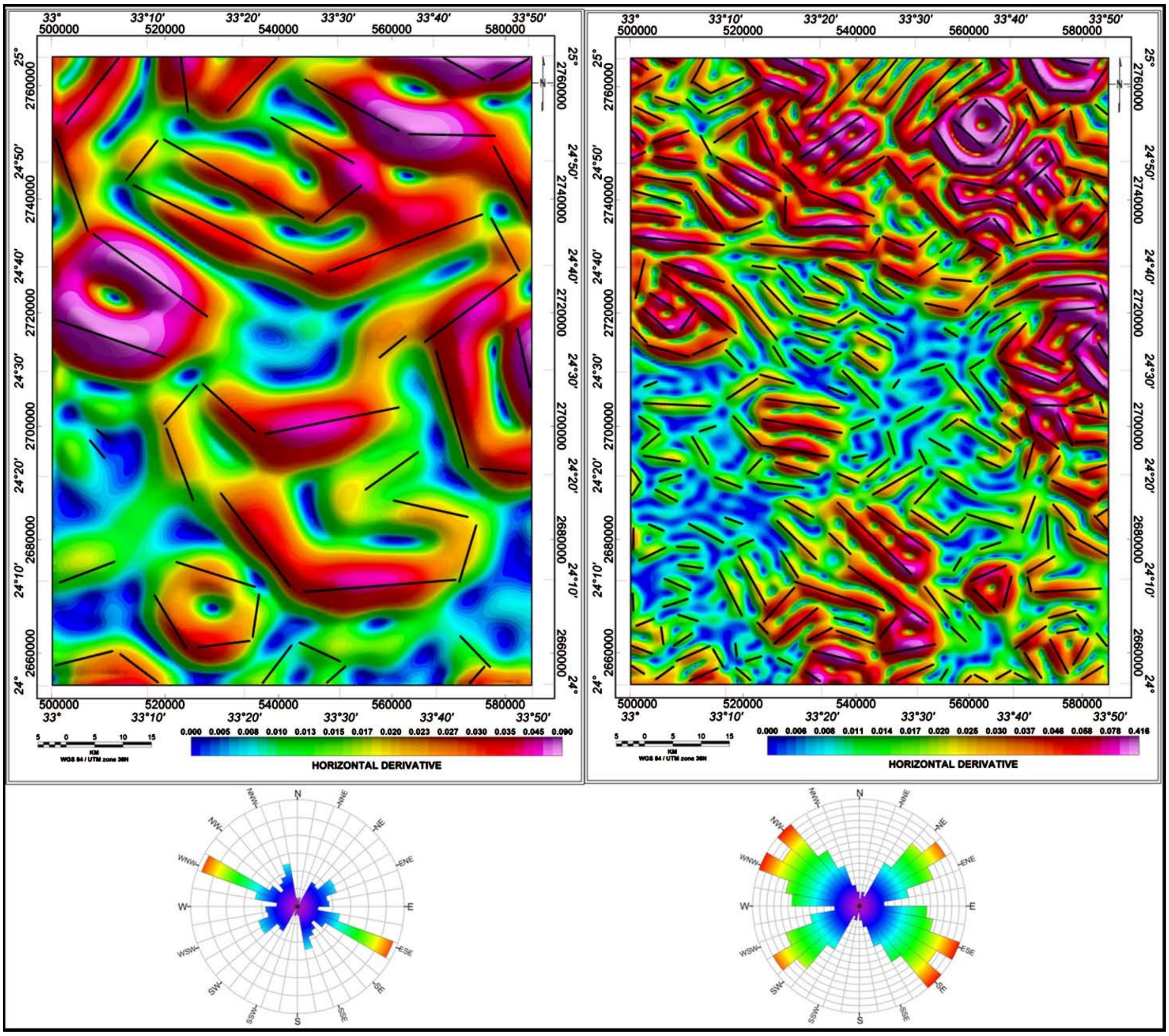

Figure 9. Basement structural lineaments trend analysis rose diagram of total horizontal derivative for both regional and residual magnetic components of Atmur Nuqra area, South Eastern Desert, Egypt.

(H7) are surrounding a sedimentary basinal area (G1). This basinal area detected at deeper depths and trending close to NW-SE direction.

The basement tectonic map (Figure 11) shows also other three high blocks; (H8 to H10) which detected along the eastern part of the area at shallow depths. At the west of these three blocks and separated from them by large basinal area (G2) with deeper depth values and another small basinal area (G4), there are other high blocks (H11 to H16). These blocks trending mainly in NW-SE direction with shallow to moderate depth values. and resulted in a trend in NE-SW direction. Blocks (H1, H11, H12, H13, H14 and H15) are surrounding another large basinal area (G3) with deeper depth values.

Comparison between the Euler depth solution map (Figure 8) and the basement tectonic map (Figure 11) shows that basinal area (G2) is the deepest basin

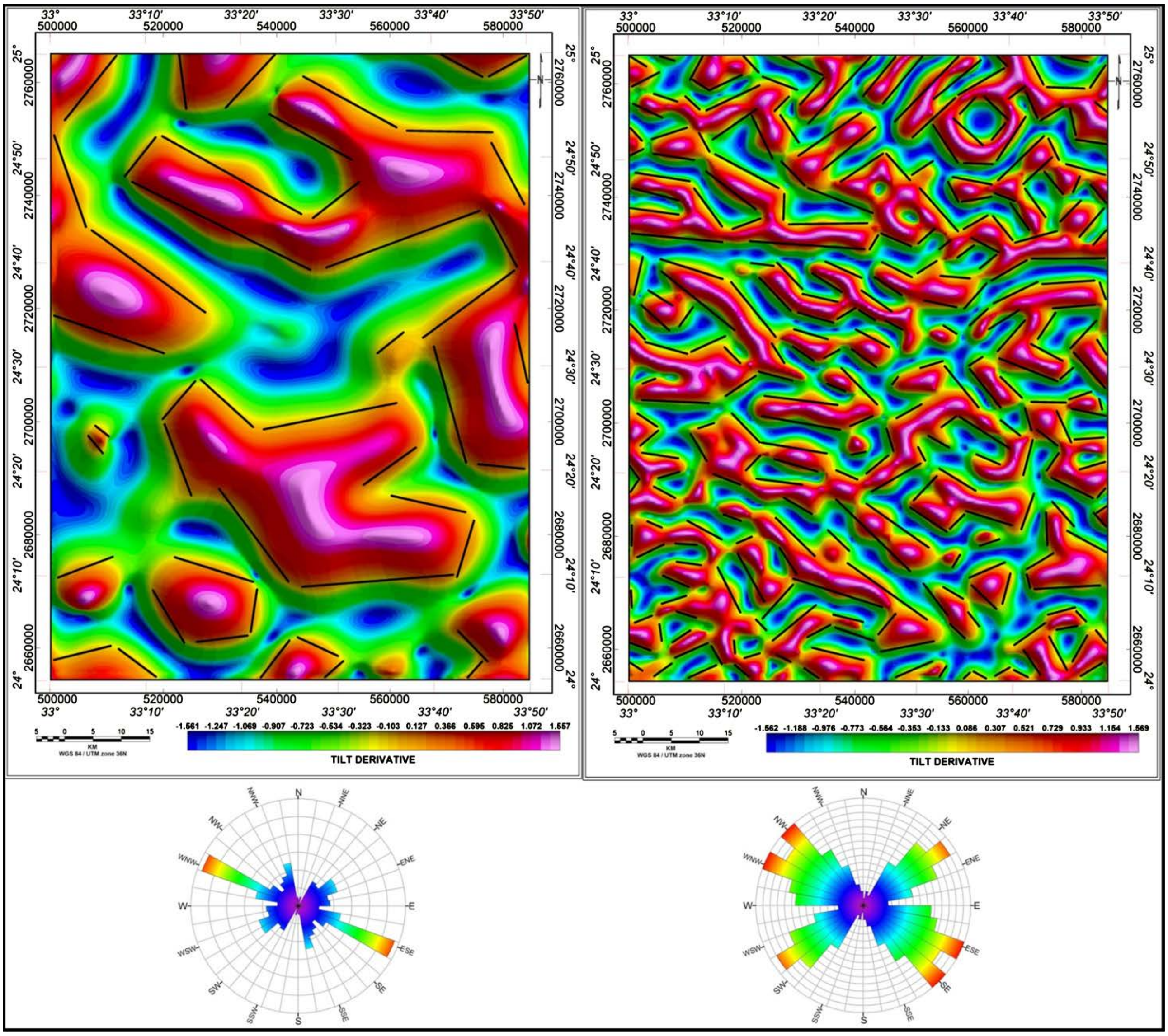

Figure 10. Basement structural lineaments trend analysis rose diagram of tilt derivative for both regional and residual magnetic components of Atmur Nuqra area, South Eastern Desert, Egypt.

all over the area with depths reach of about more than 4000 m. The second deepest basin is basinal area (G3) with depths ranging from 3500 m to 4000 m. The two basinal areas directed approximately in NW-SE direction.

4.4. Discussion of 2D-Magnetic Modeling

Two-dimensional (2D) models assume the earth is two dimensional, *i.e.*, it changes with depth (*i.e.*, the Z-direction) and in the direction of the profile (*i.e.*, the X-direction; perpendicular to the strike). 2D-models do not change in the strike direction (*i.e.*, the Y-direction). 2D-blocks and surfaces are presumed to extend to infinity in the strike direction [13].

To confirm the interpreted basement structural relief of the study area, 2D magnetic modeling was carried out along four profiles A-A', B-B', C-C' and D-D'

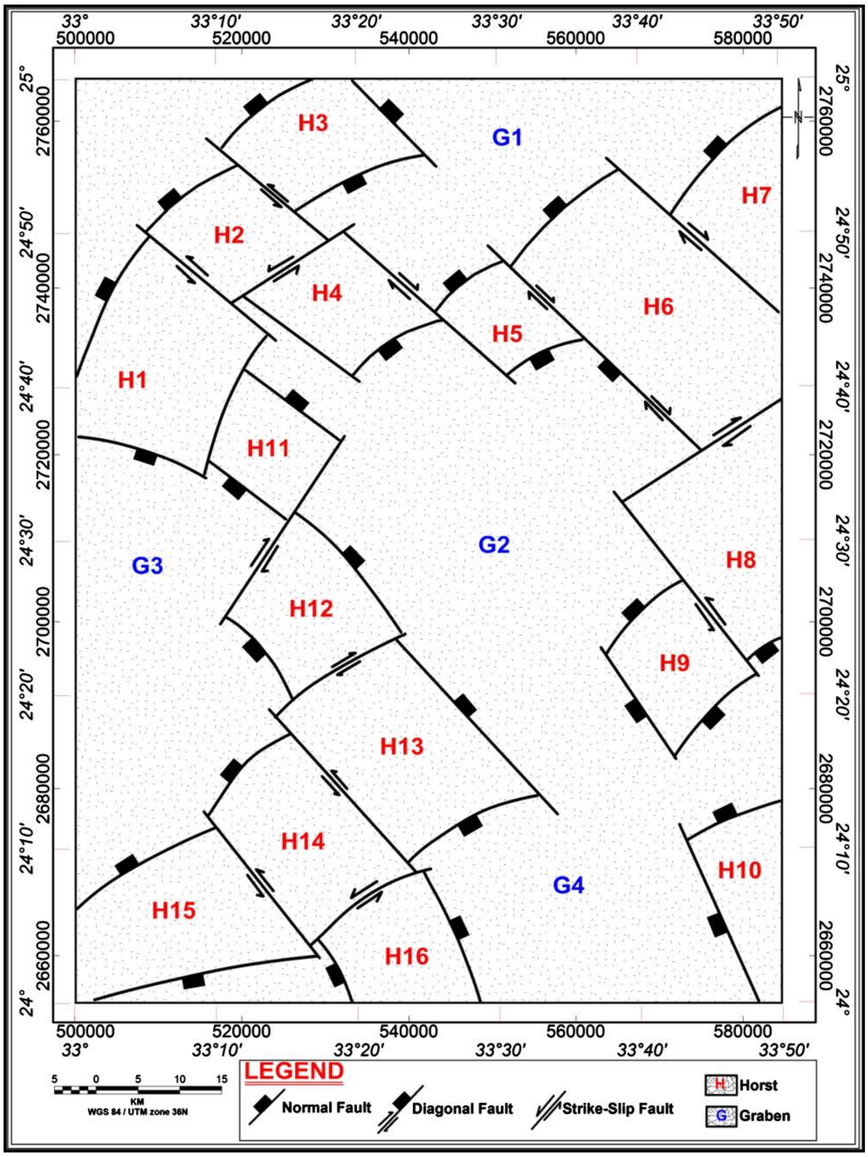

Figure 11. Interpreted basement tectonic map of Atmur Nuqra area, South Eastern Desert, Egypt.

(**Figures 12-15**) oriented in WNW-ESE, SW-NE, NNW-SSE and NW-SE trends, respectively. The magnetic susceptibility values were assumed for all rock units in the four modelled profiles.

The modeled profile (A-A') (**Figure 12**) exhibited a good fit between observed and calculated magnetic data with an error of about 3.754%. Basement rock susceptibilities were assumed and ranged from 0.01 cgs to 0.012 cgs. Profile (A-A') shows that the depth of basement at the WNW part reaches of about 400 m under the surface level whereas at the ESE part reaches of about 1800 m under the surface level. The more we go from both sides of the profile (A-A') to the middle, the depth of basement surface becomes more deep reaching at the deepest point of about 4700 m. Profile (A-A') intersected with profiles (B-B') and (C-C') at two points at the middle of the profile denoted as BB' and CC'. These two points (BB'

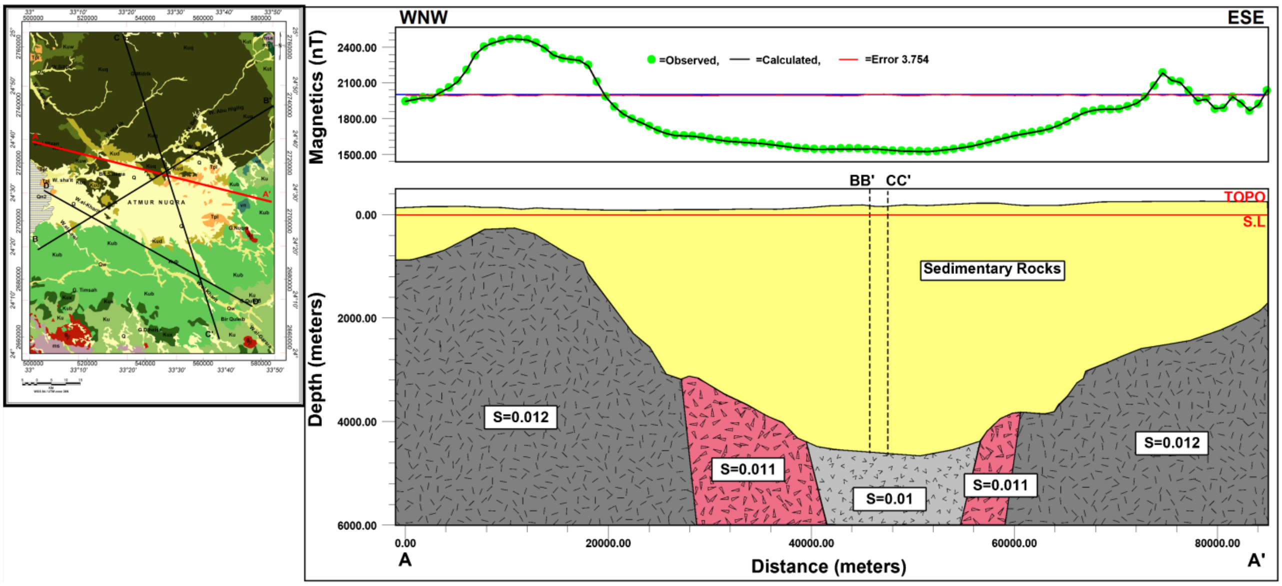

Figure 12. Two-dimensional (2D) modelled RTP magnetic profile A-A' of Atmur Nuqra area, South Eastern Desert, Egypt.

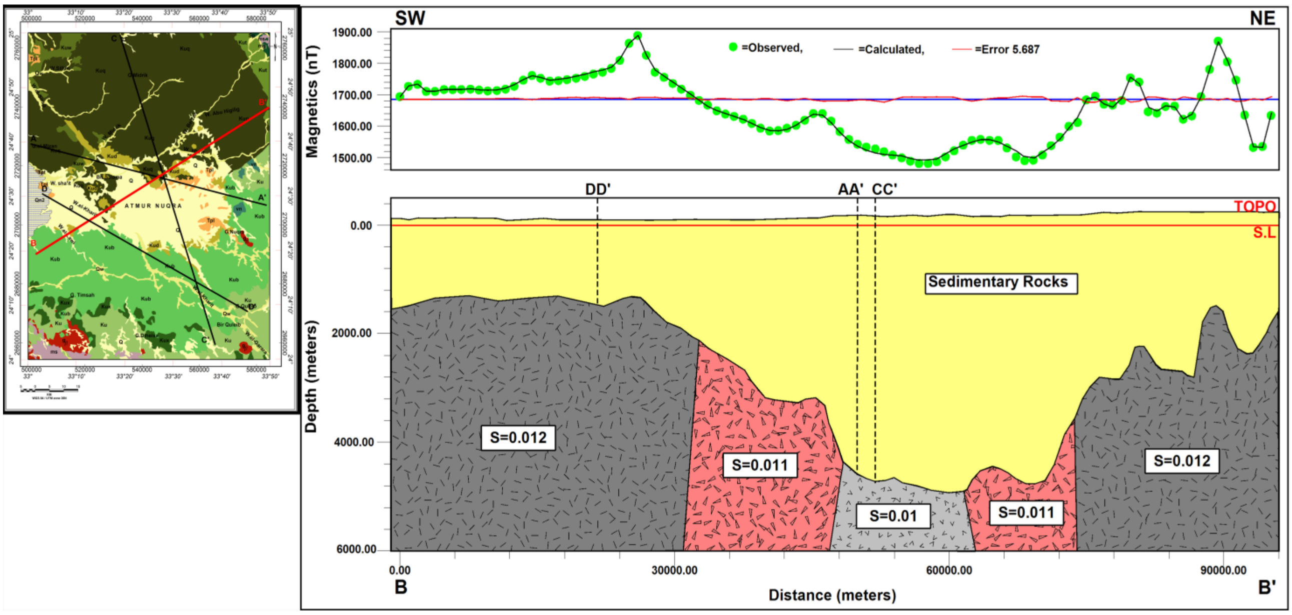

Figure 13. Two-dimensional (2D) modelled RTP magnetic profile B-B' of Atmur Nuqra area, South Eastern Desert, Egypt.

& CC') reached depth values of about 4600 m and 4570 m, respectively.

Modeled profile (B-B') (Figure 13) displayed a good fit between observed and calculated magnetic data with error 5.687%. The basement surface at the SW part of the profile (B-B') has average depth values of about 1400 m whereas the depth values reach of about 1600 m to 2200 m at the NE part of the model. The profile (B-B') gets much deeper at the middle of the profile and reaches of about 4800 m at the deepest point. The intersections between profile (B-B') and profiles (A-A', C-C' &D-D') were detected at points denoted as AA', CC' and DD' respectively. These points reached depths of about 4600 m, 4750 m, and 1450 m, respectively.

Profiles (C-C') and (D-D') (**Figure 14** & **Figure 15**) were fitted between observer and calculated magnetic data at errors 2.062% and 3.592% respectively. Basement surface depth reaches of about 2200 m at the NNW part of profile (C-C') whereas reaches of about 2950 m at SSE and the depth reaches of about 4800 m at the deepest point at profile (C-C'). At profile (D-D') the depth reaches of about 2200 m at NW part, 800 m at the middle of the profile and the deepest value 2800 m at SE part. Profile (C-C') intersected with profiles (A-A', B-B' and D-D') at three points with depth values of about 4570 m, 4750 m, and 1450 m, respectively. On the other hand, profile (D-D') intersected with profiles (B-B' and C-C') at two points with depth values of about 1450 m and 2250 m, respectively.

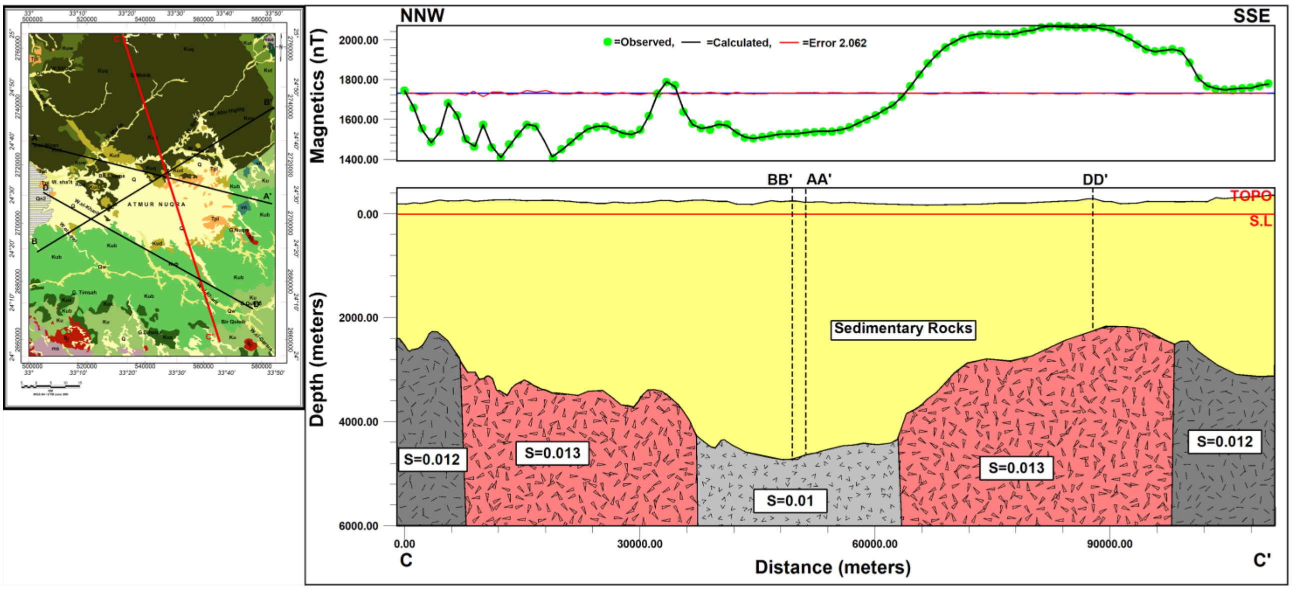

Figure 14. Two-dimensional (2D) modelled RTP magnetic profile C-C' of Atmur Nuqra area, South Eastern Desert, Egypt.

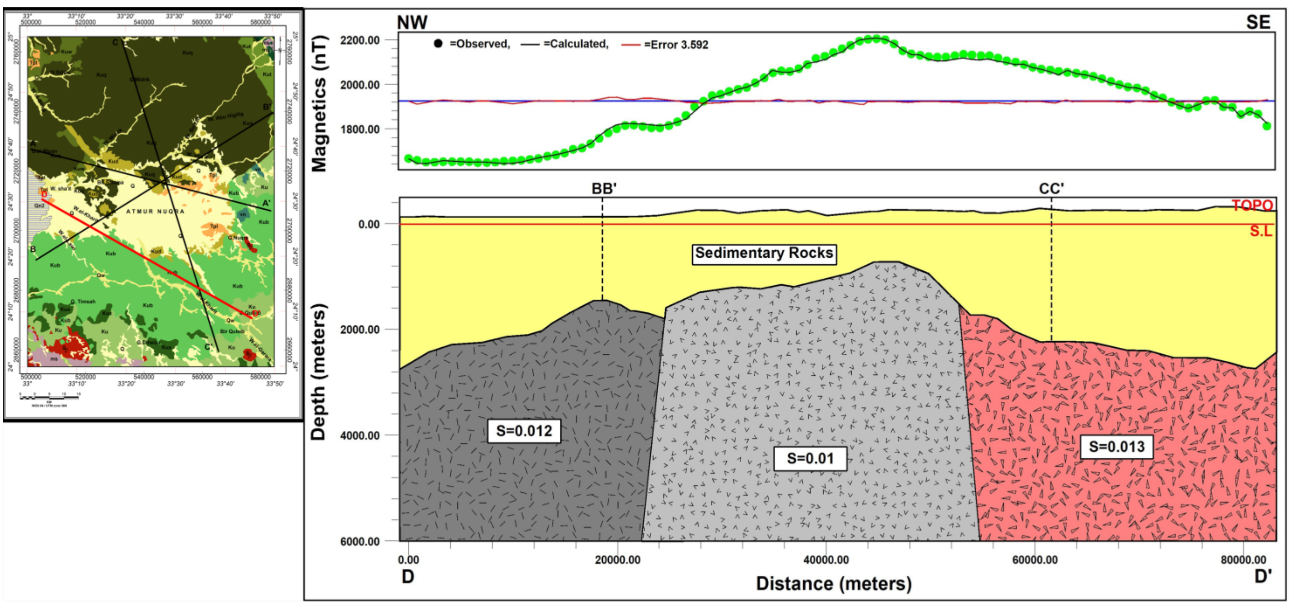

Figure 15. Two-dimensional (2D) modelled RTP magnetic profile D-D' of Atmur Nuqra area, South Eastern Desert, Egypt.

Comparing the results from 2D-magnetic modeling with the basement tectonic map (**Figure 11**) show that the basinal area (G2) is supposed to be the main sedimentary basin in the study area.

4.5. Discussion of 3D-Magnetic Modeling with Basement Tectonic Map

Another solution to the magnetic interpretation problem exists in the inversion of the magnetic data to get accurate information about the basement surface depth. Inversion refers to an automated numerical procedure that constructs a model of subsurface geology from measured magnetic data and prior information.

A model is introduced by a number of packed surface grids with average susceptibility distributions assigned for the layer underlying each surface. Calculations were performed in the wave number domain and were based on Bill Pearson's implementation of [14]. In our inversion methodology, a model of single layer with susceptibility contrasts is parameterized to describe source geometry (depth to the top). A 3D potential field modeling was carried out over the study area. **Figure 16** shows a 3D perspective of the inverted 3D depths model of the area.

Comparing the resultant inversion depth to basement with basement tectonic map (**Figure 17**) shows clearly that the area characterized by uplifts located at more than one location in the study area. The uplifted blocks at the eastern part trend mainly in N-S direction with depth values ranging from 600 m to 1000 m. Another high block was found at the south western corner of the study area trending in ENE-WSW direction with depth values ranging from 700 m to 1000 m. At the northern part of the map, there are other high blocks ranging in depth from 900 m to 1000 m and trending mainly in ENE-WSW direction and slightly

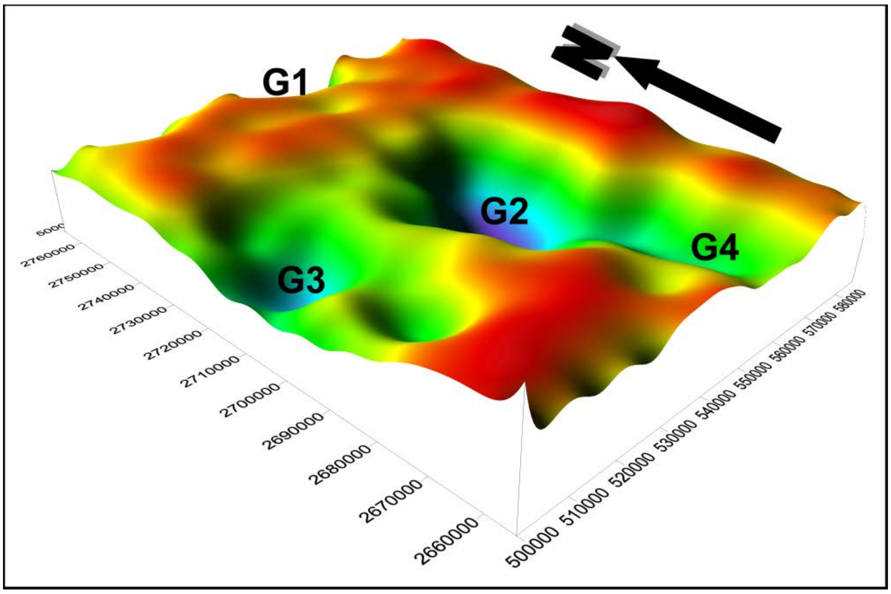

Figure 16. 3D view of result depth to basement using 3D-inversion modeling of Atmur Nuqra area, south eastern desert, Egypt.

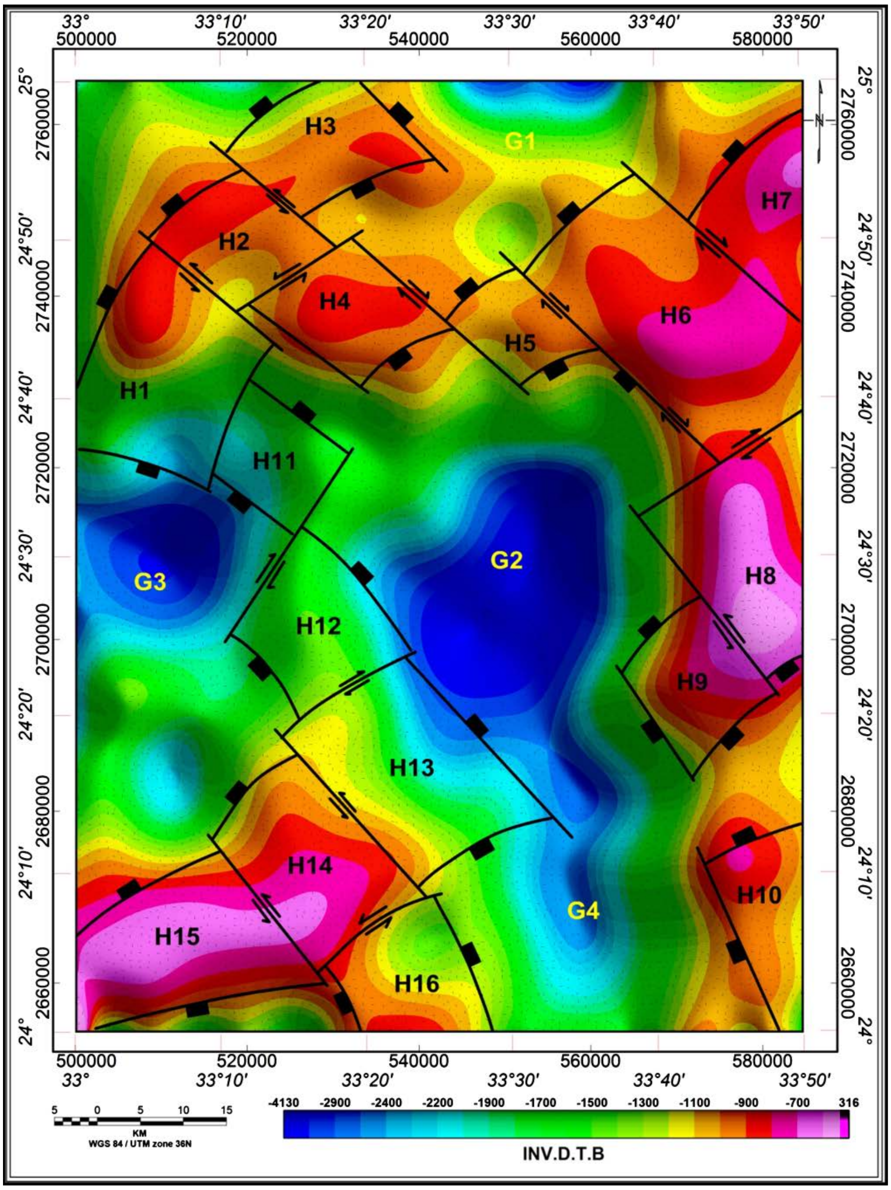

Figure 17. Basment structure superimposed on depth to basement using 3D-inversion modeling map of Atmur Nuqra area, south eastern desert, Egypt.

in E-W direction.

All the uplifted blocks surround a large basinal area at the middle of the map which ranging in depth from 2000 m to 4000 m and has a different trend: mainly NW-SE direction and slightly NNW-SSE direction. Next to west of this basinal area, there are another large basinal area trending in NE-SW direction with depth values ranging from 2000 m to 3800 m.

The inversion depth with basement tectonic map (Figure 17) shows clearly that all the basinal areas are structurally controlled by normal faults trending mainly in NW-SE and NE-SW and suffered from strike-slip movements, mainly in NNW-SSE direction and other small strike-slip movements in ENE-WSW direction.

5. Conclusions

The main purpose of this work is to determine the depth and structure of the sedimentary basin of Atmur Nuqra area. To determine the depth of the sedimentary basin Euler decnovolution, 2D-modeling and 3D-modeling techniques were applied. All the results from these techniques show that the area of study has some high blocks trending in different directions; mainly NW-SE direction and slightly in NNW-SSE and ENE-WSW directions with shallow to moderate depths ranging from 800 m to 1600 m. All the uplifted blocks surround a large sedimentary basin at the middle of the study area reaches a depth of more than 4000 m. To the west of this basin, another basin is existed with depth reaches to 3800 m.

The basement tectonic, horizontal derivative and tilt derivative maps show that the sedimentary basin area at the middle of the study area is structurally controlled through some faults and lineaments trend mainly in NW-SE and NE-SW directions, and slightly in NNW-SSE direction. The area is also affected by strike-slip movements in ENE-WSW direction.

Comparing between the basement tectonic map and 3D-magnetic modeling show that the main basin (G2) is the largest sedimentary basin in the study area.

Acknowledgements

Firstly, we thank Allah who helps us to finish this study, we also thanks to Dr/ Alaa A. F. Aref who give us the requested information about the study area and revising our manuscript. Finally, many thanks to all my colleagues who always give the help and guidance.

Conflicts of Interest

The authors declare no conflicts of interest regarding the publication of this paper.

References

[1] Shackleton, R.M., Ries, A.C., Graham, R.H. and Fitches, W.R. (1980) Late Precambrian Ophiolitic Mélange in the Eastern Desert of Egypt. *Nature*, **285**, 472-474. https://doi.org/10.1038/285472a0

[2] Said, R. (1962) Geology of Egypt. Elsevier Publ. Co., Amsterdam and New York, 293-319.

[3] El-Gaby, S. (1983) Architecture of the Egyptian Basement Complex. *Proceedings of the Fifth International Conference on Basement Tectonics*, Cairo.

[4] El-Ramly, M.F., Greiling, R.O., Kroner, A. and Rashwan, A. (1984) On the Tectonic Evolution of Wadi Hafafit Area and Environs, Eastern Desert of Egypt. In: Al-Shanti, A.M., Ed., *Proceedings of a Symposium on Pan-African Crustal Evolution in the Arabian Shield*, *I. G. C. P. No*. 164.

[5] Krőner, A. (1984) Ophiolites and Evolution of Tectonic Boundaries in the Late Proterozoic Arabian-Nubian Shield of Northeast Africa and Arabia. *Precambrian Research*, **27**, 277-300. https://doi.org/10.1016/0301-9268(85)90016-6

[6] El-Bayoumi, R.M.A. and Greiling, R. (1984) Tectonic Evolution of a Pan-African Plate Margin in Southeastern Egypt—A Suture Zone Overprinted by Low Angle Thrusting. *J. Afric. Geol*, 47-56.

[7] Ries, A.C., Shackleton, R.M., Graham, R.H. and Fitches, W.R. (1983) Pan-African Structures, Ophiolites, and Mélange in the Eastern Desert of Egypt: A Traverse at 26˚ N. *Journal of the Geological Society*, **14**, 75-95. https://doi.org/10.1144/gsjgs.140.1.0075

[8] Habeib, M.S., Ahmed, A.A. and El-Nady, O.M. (1985) Two Orogenies in the Meatiq Area of Central Eastern Desert, Egypt. *Precambrian Research*, **30**, 83-111. https://doi.org/10.1016/0301-9268(85)90047-6

[9] Conco Coral and EGPC (1987) Geological Map of Egypt, Scale 1:500,000.

[10] Aero-Service (1984) Final Operational Report of Airborne Magnetic/Radiation Survey in the Eastern Desert, Egypt. For the Egyptian General Petroleum Corporation (EGPC) and the Egyptian Geological Survey and Mining Authority (EGSMA), Aero-Service Division, Houston, Six Volumes. https://doi.org/10.1190/1.1441278

[11] Thompson, D.T. (1982) "EULDPH": A New Technique for Making Computer-Assisted Depth Estimates from Magnetic Data. *Geophysics*, **47**, 31-37. https://doi.org/10.1190/1.1442774

[12] Reid, A.B., Allsop, J.M., Granser, H., Millet, A.J. and Somerton, I.W. (1990) Magnetic Interpretation. *Geophysics*, **55**, 80-91.

[13] Geosoft Inc. (2010) Geosoft Mapping and Processing System. Geosoft Inc., Toronto.

[14] Parker, R.L. (1972) Inverse Theory with Grossly Inadequate Data. *Geophysical Journal International*, **29**, 123-138. https://doi.org/10.1111/j.1365-246X.1972.tb02203.x